

# The effect of material on bipolar membrane fuel cell performance: A review

S S Daud<sup>1</sup>, M A Norddin<sup>1</sup>, J Jaafar<sup>1</sup> and R Sudirman<sup>2</sup>

<sup>1</sup>Advanced Membrane Technology Research Centre (AMTEC), Universiti Teknologi Malaysia, 81310 UTM Johor Bahru, Johor, Malaysia

<sup>2</sup>School of Electrical Engineering, Faculty of Engineering, Universiti Teknologi Malaysia, 81310 UTM Johor Bahru, Johor, Malaysia

anam@petroleum.utm.my/juhana@petroleum.utm.my

**Abstract.** Bipolar membrane fuel cell (BPMFC) was firstly discovered in 2000 that composed of two-layered ionic conducting membranes. The importance of BPMFC development is its ability to humidify the cell when operating at a high current density that eliminates the use of the external humidification system. It is able to self-humidify the cell because of water formation at the intermediate layer from the reaction of hydrogen ion (H<sup>+</sup>) with hydroxide ion (OH<sup>-</sup>). Up to now, there is no commercial bipolar membrane (BPM) in water formation configuration for the fuel cell humidifying purpose. Thus, the researcher had come out with a composition of proton exchange membrane with anion exchange membrane by the hot-pressing method that allows them to carry the proton and anion simultaneously in a single cell. There are a few of polymeric-based PEM and AEM material had been selected for developing BPM such as Nafion, FumaPEM FAA3, quaternary ammonium polysulfone (QAPSF), and quaternary ammonium poly(phenylene)oxide (QAPPO). This review aims to determine the effect of material selection and design for developing BPM toward its performance in fuel cell based on published works. Besides, the potentialities of polymeric-based material are discussed, pointing out the main positive and negative effect of this BPM for fuel cell applications. As a case study, the use of different types of PEM and AEM material for BPM is particularly stressed, pointing out the main properties for its applications in BPMFC.

## 1. Introduction

Fuel cell is an environmental friendly electrochemical device that feed with specific fuels (i.e. hydrogen, methanol, oxygen, carbon monoxide and methane) to convert the chemical energy directly into electrical energy for stationary, traction and portable applications. The fuel cell was introduced by Sir William Robert Grove in the 19 century [1]. Generally, the fuel cell can be categorized into several types such as proton exchange membrane fuel cell, direct methanol fuel cell, solid alkaline fuel cell, molten carbonate fuel cell and phosphoric acid fuel cell according to the employed membrane/electrolyte and fed fuel [2-7]. Fuel cell based on hydrogen/oxygen (H<sub>2</sub>/O<sub>2</sub>) fuel easily to face water flooding or accumulation of water and dehydration when operate at high current discharge (0.55 A/cm<sup>2</sup>) that may damage the fuel cell and shortage it lifetime [8-12]. This problem happens because of unbalance water transportation in the membrane where electroosmotic-drag transportation exceeds back-diffusion rate at a high current discharge operation that cause accumulation of water at the electrode and gas diffusion layer, besides the membrane at anode side become dehydrate [13-14]. The suitable degree of humidification inside membrane is important for achieving high cell



performance because of water will facilitate the ion mobility across the membrane. The membrane should absorb sufficient water during operation at high current density to avoid dehydration and too much water absorption that may degrade the power output, lifetime, stability and durability. Since water management is a critical issue for fuel cell fed with  $H_2/O_2$  fuel, thus several humidification techniques have been proposed such as designing novel flow field structure [15], improving the gas diffusion layer pore structure [16], adding microporous layers [17] and etc. Basically, the humidification technique can be classified into internal humidification and external humidification. Internal humidification is involved when changing the internal fuel cell structure or composition without existing of external devices. The modification of membrane design such as combining two different ionic conducting membranes or known as BPM produces passive self-humidification behavior.

Commonly, there are two main types of membranes used in fuel cell which are proton conducting membrane or proton exchange membrane (PEM) and anion conducting membrane or anion exchange membrane (AEM). The PEM allows the positive ion to pass through the membrane, while AEM is passing the negative ion. By taking the advantage of those two membranes, the researchers had come out with BPM which is the combination of PEM and AEM to allow both ions to be transported simultaneously during operation to reduce the water flooding problem. In the past, BPM technology has been widely used in the chemical industry for various applications, including salt electrolysis, separation of mono- and divalent ions, anti-fouling, anti-deposition, water dissociation, waste recovery and cleaning products [18-19]. Recently, it was found that the BPM can be applied to the fuel cell for dissociating (electrolysis) and generating water molecules. The advantages of using BPM include the possibility of each electrode to have an optimum pH, splitting, and water generation at the cation/anion interfaces. The behavior of the BPM depends on two main factors, the bipolar junction structure between the anion and cation exchange membranes, and the nature of charge groups attached to the polymer matrix [18]. Bipolar membrane for fuel cell application (BPMFC) was firstly discovered by Unlu in 2009 consist of a BPM electrode assembly that comprised of a cathode, an anode, and BPM as shown in Figure 1 [20].

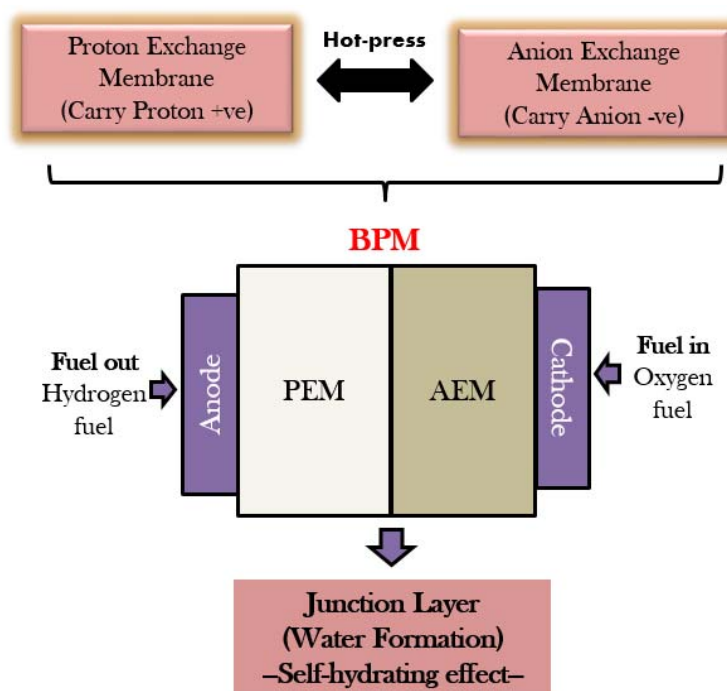


**Figure 1.** Illustration of BPMFC.

At first development stage, two configurations of BPM were prepared by Unlu and teamwork which are water formation configuration and water dissociation configuration to investigate its effect on fuel cell performance and the ability to operate at high current discharge [21]. The BPM dissociates the water into hydrogen and hydroxide ions at junction layer when the AEM has faced the anode side and PEM faces the cathode side, as illustrated in Figure 2(a). Meanwhile, to generate water molecule, the AEM should be facing the cathode side and PEM faces anode side (see Figure 2(b)). Based on Unlu experimental result, it's shown that BPM in water formation configuration ( $0.64 \text{ mW cm}^{-2}$ ) produced better power density than BPM in water dissociation configuration ( $0.03 \text{ mW cm}^{-2}$ ). The lower power density of BPM in water dissociation configuration was due to the limited amount of water transported to the AEM/PEM interface at high current density. Starting from their research works that the BPM in water formation configuration provides beneficial influence for the membrane self-humidification, thus had attracted several researchers to further the studies [22-24]. Thus, the aim of this reviewed paper was to discuss about the development of BPM in fuel cell application in term of material used, design and its effect toward cell performance and ability to withstand during high current density operation based on published studies. Besides, the BPM working principle as well as its self-humidification behavior was discussed based on simulation design and experimental result. This is the first BPMFC review study that discussed on the benefits and drawbacks of develop BPM with different design and material selection.

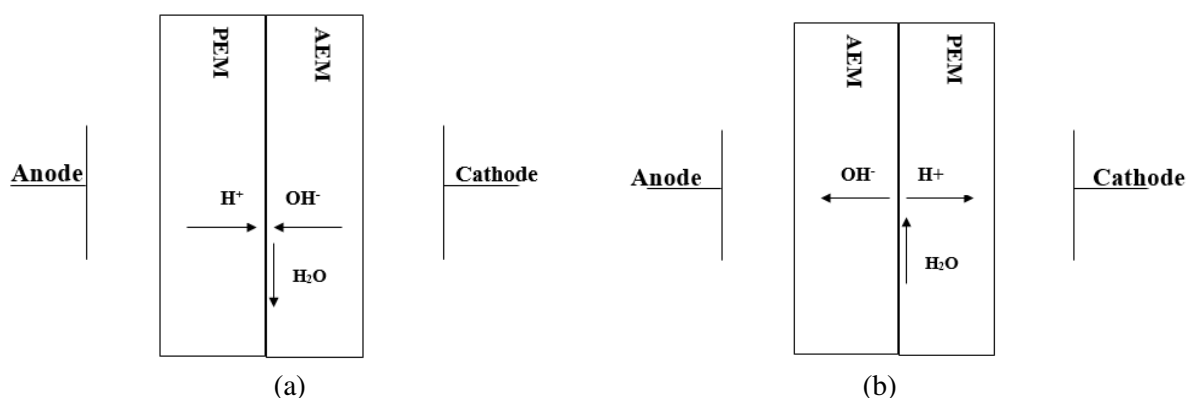


**Figure 2.** Schematic of BPM: (a) configuration of water formation and, (b) configuration of water dissociation.

## 2. Working Principle of Bipolar Membrane Fuel Cell

In this light, hydrogen fuel is fed to the anode sides while oxygen fuel is fed to the cathode sides. The BPMFC has the almost similar working principle with the proton exchange membrane fuel cell, which involves the electrochemical reaction to generate electrical energy, however, the hydroxide ion needs to diffuse the AEM before it reaches the junction layer. Figure 3 illustrates the working principle of the BPM in forming water. The hydrogen atom ( $\text{H}_2$ ) flows through the diffusion layer gas to the anode electrode. Then, the hydrogen atom is separated to proton ( $\text{H}^+$ ) and electron ( $e^-$ ) when it reaches the catalyst layer. The proton flows across the CEM toward the junction layer and the electron flow to the external circuit from the anode to produce electricity. At the same time, the oxygen atom ( $\text{O}_2$ ) flow through the diffusion layer gas to the cathode electrode. When an oxygen atom reaches the catalyst layer at the cathode side, oxygen reduction reaction occurs as a result the presence of water and produces hydroxide ions ( $\text{OH}^-$ ). The hydroxide ions will flow through the AEM toward the junction layer. At the junction layer, the hydrogen ions will react with the hydroxide ions to produce water ( $\text{H}_2\text{O}$ ), and water generation at the AEM/CEM junction will produce a self-hydrating effect. Equations (1) - (4) show the reactions that occur in the BPM.

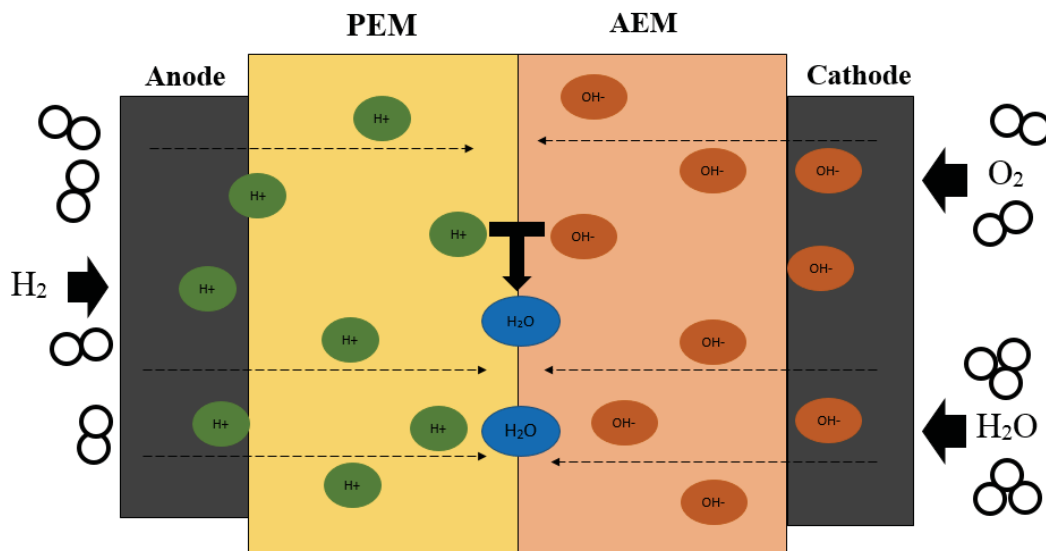


**Figure 3.** Illustration of the BPM working principle in water formation configuration.

### 3. Theoretical of Water Transport Mechanism in BPMFC

The electro-osmotic drag (EOD) and diffusion mechanism in the BPM play important roles in the transportation of water molecules for hydrating the membranes (see Figure 4). The distribution of water in the membrane depends on the balance between these mechanisms. The factors that influence the net water transport toward anode and cathode are determined by the properties of the coupling membranes, local relative humidity (RH) and electric potential [25]. The water generation at the junction is due to the reaction between OH and H<sup>+</sup> ions that are diffused toward the anode and cathode with a sufficient concentration gradient as the driving force. The half stoichiometric quantity of the water produces at the junction interface will be consumed by the cathodic oxygen reduction reaction (ORR). The EOD, specifically, the movement of water induced by moving ions leads to the accumulation of water on both sides of the PEM/AEM interface [26-27]. Self-humidification can be achieved in the BPMFC when the water produced at this interface is adequate to establish a steady water flow toward each electrode, including the water consumed by the cathode ORR. [28]. In this regard, water management, as well as the cell performance, can be enhanced by modifying the BPM fabrication procedures (i.e. membrane thickness and water uptake properties) and its pattern.

The mechanism of water transport in BPMFC has been discussed and described by researcher either via simulation or experiment, as in Peng *et al.*, [29]; Unlu *et al.* [21]; Peng *et al.*, [22]; Li *et al.*, [30]. In simulation studies, the reactions occurring in BPM have been represented by a zero-dimensional reaction kinetic model, one-dimensional steady state water transport model, and two-dimensional cross-channel configuration. Each of the models was simulated to obtain a better understanding of the water transport phenomenon in BPM.

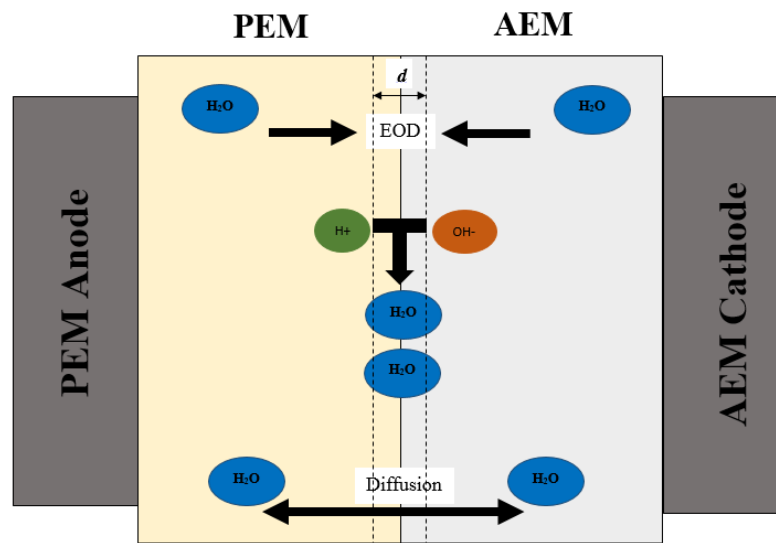
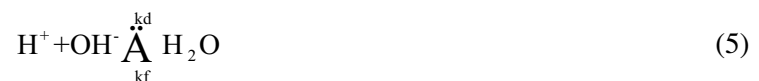


**Figure 4.** Illustration of water transport mechanism of BPMFC. ( $d$ : the width of the space charge region).

### 3.1. Zero-dimensional reaction kinetic model

It aims to represent the BPM reaction interface based on the chemical reaction kinetics and p-n junction theory. The simulation shows that the water formation reaction kinetics ( $k_f$ ) are faster compared to the water dissociation reaction kinetics ( $k_d$ ). The formation of water at the PEM/AEM interface strongly contribute to the self-humidification of the fuel cell. The fixed charges in the PEM and AEM of BPM lead to the interfacial phenomenon that forms a space charge region (SCR) between the junction zone of the PEM and AEM membrane, where the concentration of both moving ions is extremely low. It compares the electrochemical behavior of BPM junction to a semiconductor like p-n junction, where the moving positive carriers in the PEM are  $H^+$  and the moving negative carriers in the AEM are  $OH^-$  [21]. Similar to the theory of the p-n junction, the current flow at the two membrane interfaces can be categorized into two parts, which are the reaction current in the SCR and the diffusion current of the carriers in the diffusion region. The reaction of water formation and dissociation can be represented by Equation (5).



### Open Circuit Potential

The interfacial reaction of the BPMFC is in equilibrium when it operates under open circuit potential, where the interfacial potential ( $\Phi$ ) is equal to the equilibrium potential ( $\Phi_{eq}$ ) of the reaction [29]. The equilibrium formula of the BPM fuel cell is shown in Equation (6).

$$\Phi_{eq} = \frac{RT}{F} \ln(C_H^{PEM} C_{OH}^{AEM}) - \frac{RT}{F} \ln(K_w) \quad (6)$$

where,  $C_H^{PEM}$  is the concentration of the hydrogen ions in the PEM,  $C_{OH}^{AEM}$  comprises of the concentration of the hydroxide ions in the AEM,  $R$  is the ideal gas constant,  $T$  is the temperature,  $F$  is the faraday constant, and  $K_w$  (see Equation (7)) is the ion-product constant for water.

$$K_w = \exp\left(-\frac{\Delta G}{RT}\right) \quad (7)$$

$K_w$  can be expressed in mol<sup>2</sup> L<sup>-2</sup> unit,  $\Delta G$  represents the standard molar Gibbs free energy of the water dissociation reaction.

#### Steady-state Potential

Under the steady-state potential with a discharge voltage, a net reaction occurs with an interfacial overpotential of  $\eta$  in the BPM fuel cell. Therefore, the SCR including boundaries as in Equation (8), based on Boltzmann statistics, could be applied validly.

$$C_H C_{OH} = K_w \exp\left(\frac{q\eta}{kT}\right) \quad (8)$$

where,  $q$  represents the elementary charge and  $k$  is the Boltzmann constant. The interfacial potential of the BPM can be represented as  $\phi_j = \phi_{eq} - \eta$ . The potential difference in the BPM interface affects the width of SCR ( $d$ ). If the interfacial overpotential is increased, thus, the width of SCR is decrease and also reversely. The width of SCR can be determined through Equation (9).

$$d = \sqrt{2\phi\epsilon_0\epsilon_r/qN^*} \quad (9)$$

where,  $\epsilon_0$  is the vacuum permittivity,  $\epsilon_r$  is the relative permittivity,  $N^* = N_c N_a / (N_c + N_a)$  with the fixed charge densities  $N_c N_a$  in PEM and AEM. This charge affects the distribution of the SCR on PEM and AEM side of the interfaces. The water formation occurs when the interface overpotential is positive ( $\eta_f$ ), whereas the negative interface overpotential causes the water dissociation ( $\eta_d$ ) (see Equation (10) and (11)).

$$\eta_f = \phi_{eq} - \phi_j = \eta \quad (10)$$

$$\eta_d = \phi_j - \phi_{eq} = -\eta \quad (11)$$

The major carrier in the BPM is the H<sup>+</sup> in the PEM and OH<sup>-</sup> in the PEM. Meanwhile, the minor carrier is the H<sup>+</sup> in the AEM and OH<sup>-</sup> in the PEM. Same as the theory of the p-n junction, the diffusion of excess minor carrier contributes to the diffusion current at the BPM interface. There are relatively more changes in the concentration of minor carrier compared to the major carrier in the SCR boundaries. Commonly, the diffusion current does not take into account since its value does not significantly affect the result. This happens because the minor carrier is lower in concentration ( $\sim 10^{-4}$  mol L<sup>-1</sup>) and only produces small diffusion current in the BPM fuel cell. The transition state theory was applied to Equation (5) to determine the rate constant,  $K_f$  and  $K_b$  by considering the reaction current of the bipolar membrane interface. Then, the reaction current density,  $i_{\text{reac}}$ , of BPM interface is determined as in Equation (12) after overcoming the energy barrier of height  $E_f$  (forward reaction) and  $E_b$  (backward reaction). If the  $i_{\text{reac}}$  is positive in value, water formation occurs at the BPM interface. When the  $i_{\text{reac}}$  is negative in value, this indicates the water dissociation takes place at the BPM interface.

$$i_{\text{reac}} = i_0 \left\{ \exp\left(\frac{\alpha F\eta}{RT}\right) - \exp\left[-\frac{(1-\alpha)F\eta}{RT}\right] \right\} \quad (12)$$

where, the  $i_0 = F_i K_i \exp[(1 - \alpha)F\eta/RT]$  represent the exchange current density at the BPM interface. Based on the differences in the Butler-Volmer reaction rate Equation at the anode/cathode, the  $i_0$  is affected by the interfacial overpotential. This could be due to the influence of electrostatic field toward the mobility of H<sup>+</sup> and OH<sup>-</sup> ions in the SCR. However, the electrostatic field in the SCR is influenced by the variation of the interfacial overpotential.

### 3.2. One-dimensional steady-state water transport model

This model was proposed to clarify the water distribution and self-humidifying behavior of the BPM. The simulation was conducted by solving the equation of water transport for AEM and PEM and taking consideration on relative humidity states at the membrane boundaries. This suggests that the water produces at the PEM/AEM interface was distributed to each membrane's boundary via EOD and diffusion. Furthermore, the water from this source can also be used for ORR purpose. The findings from this simulation confirmed the possibility of the cell self-humidification. The phenomenon of the EOD by hydrogen in the PEM, EOD by hydroxide in the AEM, diffusion of water, and water formation reaction at the PEM/AEM interface had been taken into account in this model. Equations (13) and (14) represent the phenomenological transport of water in PEM and AEM.

$$\text{PEM:} \quad J_w = -D_c \nabla c_w + n_{d,c} \frac{1}{F} \quad (13)$$

$$\text{AEM:} \quad J_w = -D_a \nabla c_w + n_{d,a} \frac{1}{F} \quad (14)$$

where,  $J_w$  is water flux in the membrane;  $c_w$  is the water concentration in the membrane;  $D_c$  and  $D_a$  the diffusion coefficient of water in PEM and AEM;  $n_{d,c}$  and  $n_{d,a}$  are the EOD coefficient in PEM and AEM;  $i$  represent the current density and  $F$  is the Faraday constant.

The  $i$  can be equated based on Faraday and Ohm's law (see Equation (15) and (16)):

$$\text{PEM: } i = FgJ_H = -\sigma_c \nabla \phi \quad (15)$$

$$\text{AEM: } i = FgJ_{OH} = -\sigma_a \nabla \phi \quad (16)$$

where,  $J_H$  is the molar fluxes of hydrogen;  $J_{OH}$  is the molar fluxes of hydroxide;  $\sigma_c$  and  $\sigma_a$  are the ionic conductivities of PEM and AEM. The water, protons and hydroxide are conserved in Equation (17)-(19):

$$\nabla gJ_w = 0 \quad (17)$$

$$\nabla gJ_H = 0 \quad (18)$$

$$\nabla gJ_{OH} = 0 \quad (19)$$

Then, Equations (13)-(14) are combined to yield the Equations PEM and AEM for the BPM:

$$\text{PEM: } \nabla g(-D_c \nabla c_w - \frac{n_{d,c} \sigma_c}{F} \nabla \phi) = 0, \nabla g(\frac{\sigma_c}{F} \nabla \phi) \quad (20)$$

$$\text{AEM: } \nabla g(-D_a \nabla c_w - \frac{n_{d,a} \sigma_a}{F} \nabla \phi) = 0, \nabla g(\frac{\sigma_a}{F} \nabla \phi) \quad (21)$$

The rate of water generation at PEM/AEM interface,  $g$  can be determined as Equation (22):

$$g = \frac{i_{\text{reac}}}{F} \quad (22)$$

### 3.3. Two-dimensional cross-channel configuration

This model was proposed to improve the one-dimensional BPM because of the fact that the water source/sink on the PEM/AEM interface [22], water transport may be related to local reaction rate, and the multidimensional catalyst layer. The two-dimensional BPM had considered the transport in the catalyst layer and gas diffusion layer, as well as the electrochemical reactions. Three electrochemical reaction zones were involved in this configuration, which are cathode catalyst layer, anode catalyst layer, and PEM/AEM interface. In this regard, better and deeper understanding of electrochemical reaction of BPM can be achieved when the configuration is approximately close to reality. The explanation below is based on water formation reaction model, as shown in the study by Li *et al.* [30].

#### Current in Catalyst Layer

The current is split into the ionic current and the electronic current when it is in the catalyst layers, while the hydrogen and hydroxide ions pass through the ionic conductor to produce an ionic current. Meanwhile, the electrons pass through the porous carbon materials to produce an electronic current. The current conservation in the catalyst layer is expressed as Equation (23).

$$\nabla \mathbf{g}_s + \nabla \mathbf{g}_e = 0 \quad (23)$$

where,  $i_s$  represents the ionic current density and  $i_e$  represents the electronic current density.

H<sup>+</sup> and OH<sup>-</sup> ion transport:

$$\nabla \mathbf{g}_e = \nabla \mathbf{g}(-\sigma_e \nabla \phi_e) = S_e \quad (24)$$

Electron transport:

$$\nabla \mathbf{g}_s = \nabla \mathbf{g}(-\sigma_s \nabla \phi_s) = S_s \quad (25)$$

where,  $S_s$  represents the source term resulted from electrochemical reactions,  $e$  represents the electrolyte phase,  $S_e$  is the property of electron conducting phase, denotes the  $\phi_e$  electrolyte potential and the  $\phi_s$  electronic potential.

The overpotential in the catalyst layer is expressed in Equation (26).

$$n = \phi_s - \phi_e - E \quad (26)$$

where,  $E$  denotes the equilibrium potential for anode catalyst layer and cathode catalyst layer.

The source terms in the catalyst layers are:

$$\left\{ \begin{array}{l} S_e = -j \\ S_s = j \\ j = a_{v,cl} i_o \left( C_R \exp\left(\frac{\alpha_a F n}{RT}\right) - C_o \exp\left(\frac{\alpha_c F n}{RT}\right) \right) \end{array} \right. \quad (27)$$



where  $a_{v,CL}$  represents the active specific surface area of catalyst layer,  $i_o$  is the exchange current density,  $C_R$  and  $C_O$  denoted the reduced and oxidized species concentration correction factors,  $\alpha_a$  and  $\alpha_c$  are the respective transfer coefficients.

#### Current in PEM, AEM, Gas Diffusion Layer (GDL), and Microporous Layer (MPL)

Equation (28) shows the current density in the GDL and MPL based on the Ohm and Faraday law. Meanwhile, the current density for AEM, PEM and at PEM/AEM interface are expressed earlier as in a one-dimensional model.

$$i_s = -\sigma_s \nabla \phi_s \quad (28)$$

where  $\sigma_s$  represents the electronic conductivity.

The active specific area of the PEM/AEM interface,  $a_{v,scr}$  is considered in calculating the water consumption at the PEM/AEM interface for two-dimensional model (see Equation (29)), but not in a one-dimensional model.

$$g = \frac{a_{v,scr} \cdot i_{react}}{F} \quad (29)$$

#### 4. Polymeric-based Material of Ionic Conducting Membrane

Since in 1950s, the functionality of ionic conducting membrane in electrochemical application had been studied. Ion conducting membranes are sheets or thin films of ion conducting material which able to permit of cations/proton or anions and split the ions [31-32]. Development of ionic conducting membrane in terms of material and fabrication had increased from year to year for improving the chemical stability, mechanical strength, thermal stability and electrical resistance. Generally, the ion conducting membrane consists of hydrophobic substrates, movable counter-ions (mobile ions) and immobilized ion-functionalized groups (fixed charge ion groups) [33-34]. The classification of ionic conducting membranes determines, based on the attachment of fixed charged ion groups either cation or anion onto material backbone. The cation/proton conducting membrane comprised of a fixed negative charge ions that only permit positive ion to across it while repelling the negative charge ion. Meanwhile, the anion conducting membrane consists of a fixed positive charge ion, thus it only allows negative charge ion to across it while repelling positive charge ion. Ionic conducting membrane based on polymer material is well-known in fuel cell application due to its excellent in thermomechanical stability. The term “polymer” comes from Greek words which is a combination of poly (many) and meros (many parts) [35]. The classification of polymeric materials is poly(perfluorosulfonic acid), non-poly(perfluorosulfonic acid) and natural polymer.

The studies of promising material for BPM is still in early development stage as only limited published works can be found. Due to BPMFC studies only used commercial Nafion membrane as PEM, thus this reviewed will only discuss on this material. Up to now, the researchers only focused on selecting promising material for AEM of BPM due to the commercial AEM membrane, FUMAPEM FAA-3 exhibits poor performance (power density: 8 mW/cm<sup>2</sup>) when composed with Nafion. Among of the selected AEM for BPM are QAPAES, QAPPO, quaternary benzyl trimethylammonium PPO, and QAPSF.

#### Proton Conducting Material for Bipolar Membrane Fuel Cell

The Nafion membrane is a well-known poly(perfluorosulfonic acid) proton conducting membrane for fuel cell application. Walther Gustav Grot is a first person that discovered the Nafion membrane in the late 1960s and commercialized by DuPont in 1970s [36-37]. Till today, Nafion membrane has been

the most promising membrane for fuel cell due to their high electrochemical properties as well as excellent chemical stability. Nafion consists of polytetrafluoroethylene backbone and is made with perfluorinated vinyl ethers pendant side chains terminated by a sulfonate ionic group [38-40]. As reported by Mauritz and Moore the morphological structure of Nafion are [41]:

- i. Nafion phase consists of distinct hydrophobic and hydrophilic channels.
- ii. The hydrophilic sites consist of sulfonate groups which able to swell or shrink depending on water absorption.
- iii. The hydrophobic channels consist of tetrafluoroethylene backbone and perfluorovinyl ether pendant side chains which provides excellent mechanical stability, chemical stability and thermal stability.

Figure 5 shows the chemical structure and matrix of Nafion. Up to now, there are a few types of Nafion had been developed which are Nafion 115, Nafion 117, Nafion 211 and Nafion 212. The Nafion are named according to its denoted number where (1) polymer equivalent weights – first two digits, (2) membrane thickness in 1/1000 inch – third digits [42]. So, the Nafion 117 is 7 mil in thickness and had polymer weight about 1100 g/mol. The equivalent weight represents the ratio of polymer in grams per mole of sulfonic acid groups. The transport and mechanical properties of Nafion is depending on the equivalent weight of polymer where the increasing equivalent weight (reduction in sulfonation degree) will improve the mechanical properties but decreasing proton transportation. Usually Nafion having 1100 g/mol was selected for H<sub>2</sub>/O<sub>2</sub> fuel cell application which obtain fair balance between proton conductivity and mechanical properties [36]. Although the Nafion is almost perfect membrane for fuel cell application, but it still has some weakness which is expensive, high hydrogen crossover, and suitable for low-temperature operation where at high-temperature the dehydration will occur [43-50]. But, undeniable that the Nafion is still the promising material for H<sub>2</sub>/O<sub>2</sub> fuel cell with superior performance.

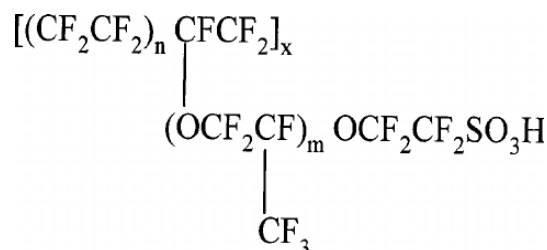


**Figure 5.** Chemical structure of Nafion membrane.

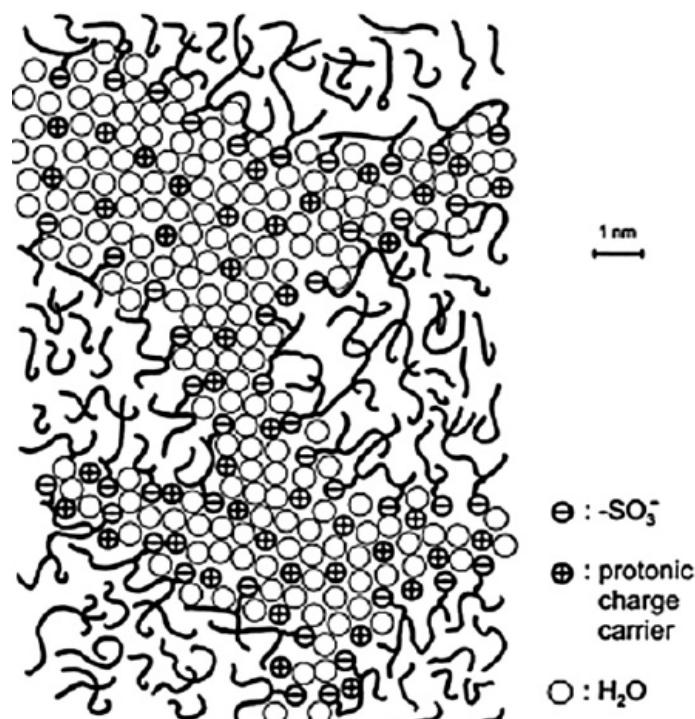


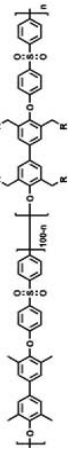
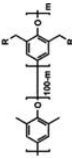
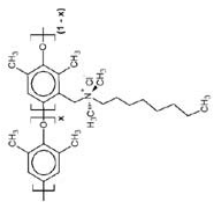
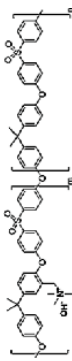
**Figure 6.** The hydrophobic and hydrophilic separation sites in the microstructure of Nafion [51].

### Anion Conducting Material for Bipolar Membrane Fuel Cell

The role of anion conducting membrane in BPMFC is to pass through the hydroxyl ion to the intermediate layer. Up to now, there are several polymers such as PAES, PPO, and PSF had been modified as AEM. Among of the polymer modification method are via chloromethylation-functionalization (CF) whereby the cationic functional group such as quaternary ammonium [53-55], quaternary phosphonium [56-60], imidazolium [61-66], sulfonium [67-69], and guanidium [70] are introduced onto the polymer backbone in order to change the nature of pristine polymer into alkaline. At first, the pristine polymers were chloromethylation with chloromethyl agent such as chloromethyl methyl ether ( $\text{C}_2\text{H}_5\text{ClO}$ ), chloromethyl octyl ethers ( $\text{C}_8\text{H}_{17}\text{ClO}$ ) and bis(chloromethyl) ether ( $(\text{CH}_2\text{Cl})_2\text{O}$ ) to introduce chloromethyl group ( $\text{CH}_2\text{Cl}$ ) onto the backbone. Since, these chloromethyl agents are carcinogenic and hazardous chemicals, thus as an alternative through in-situ technique that introduced for the first time in 2013 by Jasti *et al* [71] using a lewis acid catalyst, paraformaldehyde and trimethylchlorosilane were used. Then, the chloromethylated polymer was further functionalized with the required cationic group to develop AEM.

The properties of CF AEM membrane highly depend on the degree of CF, where high CF produces high anion conductivity while low CF produce low anion conductivity. However, the degree of CF should be controlled at an optimal level because the too high degree of CF causes serious membrane swelling that lead to loss of membrane mechanical property. The degree of CF determines the amount of cationic functional group attach on polymer backbone. The parameter of CF likes temperature, reaction time, acid concentration and polymer content play important to achieve the desired degree of CF. Compared to other cationic group, the quaternary ammonium mostly prefers to be functionalized with chloromethylated polymer due to relatively easy preparation and good stability [72]. The quaternary ammonium AEM produces better chemical and thermal stability compared to quaternary phosphonium and sulphonium [73]. Almost all of the reported BPMFC study used quaternary ammonium AEM to be composed with Nafion to produce high stability bipolar membrane. Table 1 summarizes the types of AEM that had been used in BPMFC studies.

**Table 1.** Reported AEM in BPMFC studies.

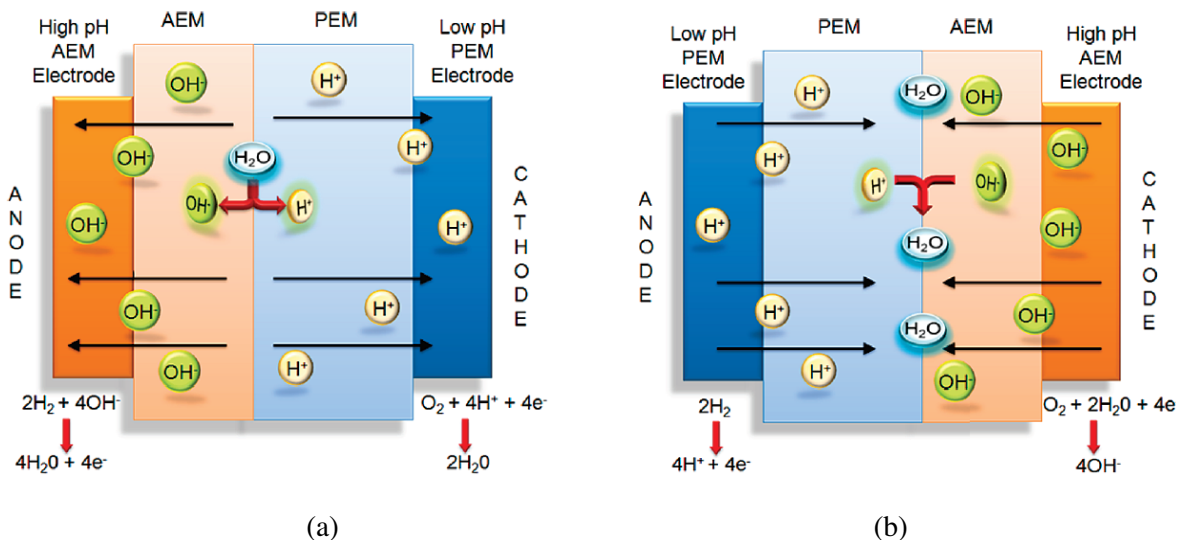
Type of AEM	Chemical Structure	Properties	Performance	Reference
Quaternary ammonium poly(arylene ether sulfone) (QAPAES)		<ul style="list-style-type: none"> <li>• High water uptake</li> <li>• Worse swelling degree</li> <li>• Poor chemical stability</li> <li>• Moderate mechanical stability</li> <li>• Promising anion conductivity</li> </ul>	<ul style="list-style-type: none"> <li>• Anion conductivity: 21.2 mS/cm</li> </ul>	[21]
Quaternary ammonium poly(2,6-dimethyl 1,4-phenylene) oxide (QAPPO)		<ul style="list-style-type: none"> <li>• Excellent alkaline stability</li> <li>• Moderate water uptake</li> <li>• High thermal stability</li> <li>• Excellent mechanical strength</li> <li>• Promising performance</li> </ul>	<ul style="list-style-type: none"> <li>• Peak power density: 294 mW/cm<sup>2</sup></li> </ul>	[24]
Quaternary benzyl trimethylammonium polyphenylene oxide		<ul style="list-style-type: none"> <li>• Moderate water uptake</li> <li>• Low swelling degree</li> <li>• Excellent chemical and mechanical stability</li> <li>• Promising anion conductivity</li> </ul>	<ul style="list-style-type: none"> <li>• Anion conductivity: 40 mS/cm</li> </ul>	[74]
Quaternary ammonium polysulfone (QAPSF)		<ul style="list-style-type: none"> <li>• Excellent alkaline stability</li> <li>• Long cell lifetime</li> <li>• High anionic conductivity</li> <li>• Excellent mechanical strength</li> </ul>	<ul style="list-style-type: none"> <li>• Anion conductivity: &gt;10-2 S/cm</li> <li>• Peak power density: 50 mW/cm<sup>2</sup></li> </ul>	[22]
Commercial FUMAPEM FAA-3	Not state	<ul style="list-style-type: none"> <li>• Low resistance</li> <li>• High selectivity</li> <li>• High alkaline stability</li> <li>• Moderate performance</li> </ul>	<ul style="list-style-type: none"> <li>• Peak power density: 30 mW/cm<sup>2</sup></li> </ul>	[23]

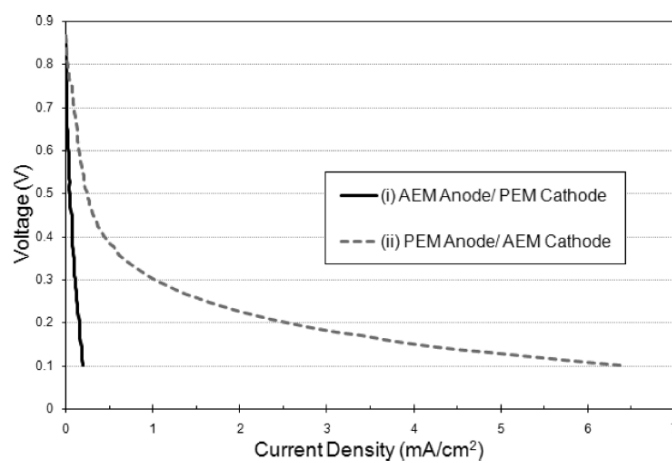
## 5. Effect of Material on Performance of Bipolar Membrane Fuel Cell

### 5.1. Nafion 212-Quaternary ammonium poly(aryl ether sulfone) bipolar membrane

The early development of BPM started in 2009 by Unlu *et al* [75]. At first, Unlu and teamwork had designed two BPM configuration which is (1) water formation configuration, were composed of PEM anode/AEM cathode and (2) water dissociation configuration were composed of AEM anode/PEM cathode (see Figure 7a and 7b) in order to determine the effect presence of water molecule at the junction layer toward cell performance. They had chosen Nafion 212 as PEM to be composed with QAPAES as AEM for developing bipolar membrane via hot-pressed method. At first, PEM half-cell and AEM half-cell were prepared by pressing together electrode with AEM at a 2MPa gauge pressure and room temperature for 3 minutes, while PEM pressed with electrode at a 2MPa gauge pressure and 135 °C for 3 min. Then, the two half –cell were pressed together at 2 MPa and room temperature for 5 min. The total thickness of Nafion 212-QAPAES BPM is 174  $\mu\text{m}$ .

Based on I-V polarization curve in Figure 7(c), the BPM in water dissociation configuration exhibit 0.03  $\text{mW}/\text{cm}^2$  for peak power density and 860 mV for open circuit voltage. In this BPM configuration, the hydrogen oxidation takes place at the anode under alkaline environment, yet produce water. Meanwhile, the oxygen is reduced at the cathode which produce protons and resulting in water formation as in Figure 7(a). Then, the  $\text{OH}^-$  moves across the AEM toward the anode and  $\text{H}^+$  moves across the PEM toward the cathode. The depletion layer at the junction contribute to junction potential. Meanwhile, the BPM in water formation configuration exhibits 867 mV of open circuit voltage and 0.64  $\text{mW}/\text{cm}^2$  of peak power density, which is higher than the BPM in water dissociation. In this configuration, hydrogen is fed at the PEM anode, while oxygen is fed at the AEM cathode. The proton mobilizes from anode across PEM toward the junction layer and at same time anion mobilize across AEM toward the junction layer. Reaction of the proton and anion at the junction generates water. The formation of water at junction layer produce larger current and power than water dissociation that quickly leads to membrane drying.





(c)

**Figure 7.** Operation mechanism of BPMFC in different configuration: (a) water dissociation configuration; (b) water formation configuration and (c) polarization curves [21].

Another report by Unlu *et al.*, in 2010 [75] was investigating the effect of relative humidity, ionomer content in the anion-conductive electrode and inlet gas flow rates by using same PEM and AEM materials. They had found that the cell performance increased at low relative humidity compared to a single proton exchange membrane fuel cell that confirm the self-humidifying behavior of the membrane when water produce at the junction layer. However, the flooding was occurring at the electrode layer when the gas feed at high rates. In this follow-up study the Nafion 212-QAPAES able to operate at 200 mA/cm<sup>2</sup> of maximum current density in steady-state operation using dry hydrogen and oxygen fuel at 80 °C. Their developed BPM material is failing to operate at high current discharge (550 mA/cm<sup>2</sup>) due to excessive “self-hydration” and flooding at the cathode when dry H<sub>2</sub>/O<sub>2</sub> used as the current discharge increased more than 200 mA/cm<sup>2</sup>.

### 5.2. Nafion-FUMAPEM FAA-3 bipolar membrane

Motivated from previous study that the water flooding in the cell is still occurring when current discharge is increased, thus Weida *et al.*, [23] had come out with composing Nafion with FUMAPEM FAA-3 and porous hydrophilic membrane as the bipolar membrane (see Figure 8). The thin, porous, and hydrophilic membrane was used between PEM and AEM where the hydrogen ions and hydroxide ions will react within the water in the pores of this membrane. Then, the water forming in the thin membrane was shunted out externally from the cell which solving the water flooding problem. The Toray TGP-H-030 (non-PTFE treated, 110 μm thick carbon paper) was used as the supported intermediate membrane. The BPM electrode assembly was prepared by hot-pressed the anode with Nafion and supported membrane at 135 °C and 2000 psi for 3 minutes. Then, the PEM half-cell pressed with FUMAPEM FAA-3 and the cathode at 2000 psi and 60 °C for 5 minutes. They reported that the developed BPM exhibit only 8 mW/cm<sup>2</sup> of maximum power density, which is lower than single cell PEM (750 mW/cm<sup>2</sup>) and AEM (30 mW/cm<sup>2</sup>). The possible reason for this poor BPMFC performance is due to additional of the supported porous membrane that cause an increase of electrolytic resistance. Although this BPM exhibit poor cell performance, but interestingly it able to operate effectively without flooding when feed with 100% humidified gas streams and discharged at 50 mV at 30 °C. The addition of supported membrane had well remove the water inside the membrane to avoid water flooding. However, the challenges remain in enhancing the BPM performance to optimal levels.

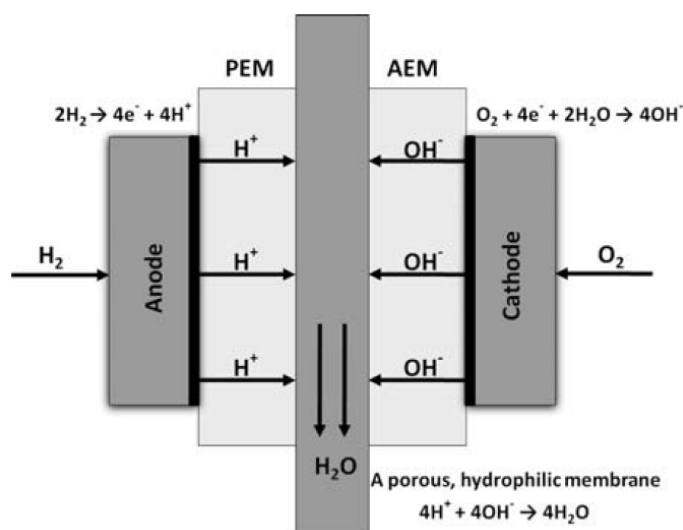


**Figure 8.** Schematic diagram of the Nafion-FUMAPEM FAA3 with intermediate membrane for BPMFC [23].

### 5.3. Nafion 211-Quaternary benzyl trimethylammonium polyphenylene oxide bipolar membrane

Arges and coworkers [24] had developed BPM using Nafion 211 as PEM and quaternary benzyl trimethylammonium polyphenylene oxide as AEM. Based on their previous study, the PPO was selected instead of PSF and PAES because it exhibits better ionic conductivity [24]. The PPO backbone was attached to quaternary benzyl trimethylammonium bromide groups. At first, the PPO brominated at 0.33 of the degree of functionalization to the benzyl position and 0.20 to the aryl position. The *n*-bromosuccinimide and azobisisobutyronitrile was used as brominating reagent and free radical initiator for synthesizing brominated PPO. Adding of bromine to the benzyl position is crucial due to this moiety undergoes nucleophilic substitution with an amine to produce quaternary ammonium groups [76]. The presence of bromine in PPO aryl position increased the hydrophobicity behavior of AEM which improved ion exchange capacities without excessive water uptake [77]. In this study, the influence of the PEM thickness toward  $\text{H}_2/\text{O}_2$  fuel cell was investigated. It found that the thinner PEMs produce better cell performance due to lower ohmic overpotentials and smaller resistivity especially when operate at high current discharge. The Nafion 211-quaternary benzyl trimethylammonium PPO BPM exhibits poor cell performance due to incompatibility PEM and AEM material. The reason is due to different ability of membrane in absorbing water where the PEM absorbs large water while AEM absorb only little water as it had hydrophobicity behavior. Thus, the PEM facing worse swelling when current discharge increase, which lead to poor contact between the PTFE backbone in Nafion and the hydrocarbon PPO backbone. Poor contact contributes to dielectric gaps which is likely bubbles or air gaps. They recommend the used of all hydrocarbon materials for membrane to increase the degree of entanglement between AEM and PEM as well as increase the cell performance. Besides, the less hydrophobic material of AEM also suggests to increase the ionic conductivity in the future work.

### 5.4. Nafion 117-QAPPO bipolar membrane

In 2015, Clure *et al* [74] had focused on improving the contact between PEM and AEM to increase the porosity and the degree of entanglement by introducing electrospun nanofiber mats for the bipolar junction layer. The electrospun fibers were prepared by pumping solutions via a 10 ml syringe fitted with a 22-gauge needle. The parameter of electrospinning was varied in term of applied times (~30 min to 2 h) and voltage (~8-20 kV). Three types of polymers were electrospun which are filler polymers such as PSF and polyacrylonitrile (PAN), and functionalized polymers like chloromethylated PSF and Nafion 117 ionomer solution. Besides, big attention also given to AEM materials where the

PPO was functionalized with long-chain alkyl amine groups consisting various chain lengths. The alkyl chain length varied into  $n=4$ ,  $n=6$  and  $n=8$  with two different degrees of functionalization (31% and 45%). It was reported that the  $n8$ -PPO at 45% degree of functionalization exhibits the highest anion conductivity (28.4 mS/cm) with low water uptake (15.8%). Figure 9 shows the scanning electron microscope (SEM) images for the cross-section of BPM with and without junction layer. Both of the BPM shows intimate overlap for each other. Based on ionic conductivity results, the BPM with junction layer ( $\sim 10$  mS/cm<sup>2</sup>) exhibits better ionic conductivity than no junction layer (7.5 mS/cm<sup>2</sup>) due to increase the degree of entanglement.

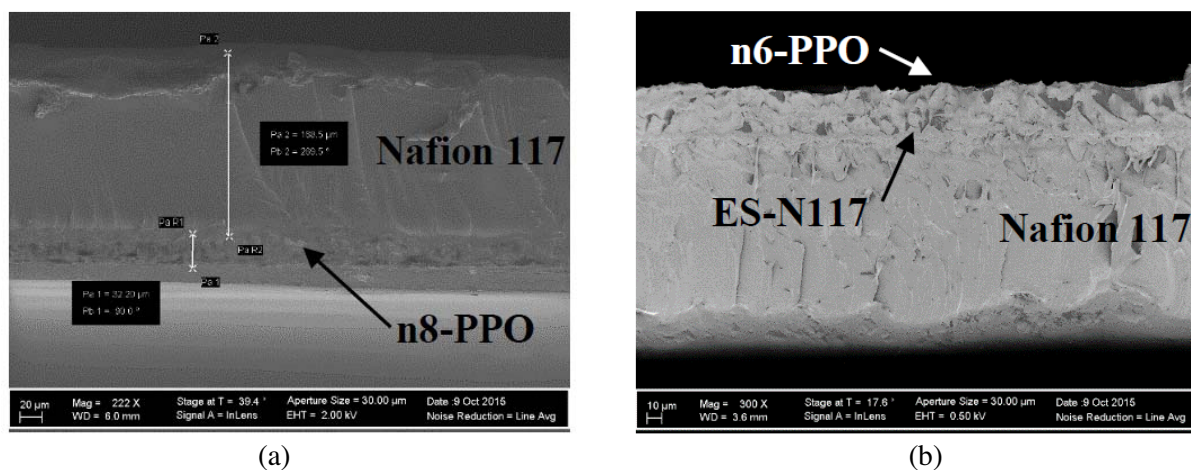


**Figure 9.** Scanning electron microscope images of (a) BPM without junction layer and (b) BPM with an electrospun junction layer [74].

### 5.5. Nafion 117-QAPS bipolar membrane

Recently, Peng *et al.*, [22] had prepared BPM by pressing together of Nafion 117 with QAPS (thickness:  $11\mu\text{m}$ ) membrane at  $60^\circ\text{C}$  and 4 MPa for 10 min. They had select QAPS as AEM due to it had excellent mechanical strength, thermal stability, ionic conductivity and good stability for long-term operation. The effect of AEM thickness was conducted through simulation where its influence the required water amount in the junction layer for obtaining effective water diffusion to take place in the anode and cathode. The high peak power density ( $327\text{ mW/cm}^2$  at 323 K) of BPM was achieved in this study. The Nafion 117-QAPS was tested under dry  $\text{H}_2/\text{O}_2$  at 303 K and 50/80 SCCM for prolonged periods. It had found that the BPM managed to operate successfully without flooding hours for 40 hours with no sign of degradation. Based on ATR-FTIR analysis, the normalized O-H stretching, vibration intensity was found when Nafion 117-QAPS operated at  $70\text{ mA/cm}^2$  where represent the existence of water content at the junction layer. Under load operating conditions, the ionic conductivity of BPM increases gradually with decreasing cell voltage. In contrast, the BPM ionic conductivity measured in water mode is fairly independent of cell voltage (cite). This validated that the water formation of the junction layer is the main source to self-humidification. Besides, when the cell voltage is lower than 0.8 V, the measured ionic conductivity of BPM in discharge mode exceed that of water mode and the effect of self-humidification becomes evident. Thus, it clearly showed that the importance of control water generation and distribution to obtain proper water management.

## 6. Conclusion and Future Perspectives

Water flooding has become a bigger issue in monopolar PEM and AEM when operated at a high current density. Many alternatives have been suggested to overcome this issue. The use of external humidifier causes cell system to become more complex and increase the cost. A recent study found that bipolar membrane, which is the combination of alkaline-based membrane and acid-based



membrane, could potentially humidify the membrane to keep it hydrated as it is being operated at high current density. However, there is a limited number of studies conducted on this since the fuel cell applications of BPM technology are still new. The experimental study and simulation have been done to obtain a clear understanding on the principle of water transport in BPM and how it acts as a humidifier for the cell. The simulation model of BPM was developed from zero-dimensional BPM model to one-dimensional BPM model and two-dimensional BPM model, and an experiment was conducted to validate the model. Much of polymer based membrane has been selected for determining the best, most suitable and good compatibility to each other in obtaining optimal cell performance. Up to now, the high performance of BPMFC is found from Peng *et al.*, study with  $327 \text{ mW cm}^{-2}$  of power density. Challenges remain in improving the cell performance and determining the relative importance of the AEM and PEM conductivity, and the thickness, porosity, stability of membrane for long term operation, and compatibility between PEM and AEM. In the future work, the following recommendations should be considered for optimizing the BPMFC performance such as:-

- Homemade cation exchange membrane

Previous research of BPMFC has given little attention to the materials used for PEM compared to AEM. The homemade PEM should be used to replace the Nafion membrane to achieve better power output, enhance water management and cut the cost. Although the Nafion membrane is excellent in thermal and mechanical stability, but it is still limited due to its high cost, high hydrogen crossover, fast dehydration, hydroxide radical attack, and high water dependence for efficient operations. The sulfonated poly(ether ether ketone), sulfonated poly(arylene ether sulfone), and sulfonated poly(imide) is among of the suitable polymer based membrane to be used for PEM instead of Nafion. Besides of easy processing in the laboratory, these polymer-based materials also demonstrate excellent mechanical, thermal, chemical and electrical properties.

- Determine the compatibility between PEM and AEM

It is imperative to investigate the compatibility between PEM and AEM before preparing a bipolar membrane. In this light, the compatibility of the membranes can be determined based on the properties of the membranes itself. As mentioned in Peng *et al.*, [22], the water uptake of PEM should match the AEM to facilitate the formation of self-humidification. Moreover, Peng *et al.*, [22] found that the combination of Nafion with the QAPS has a better power output compared to others, The reason is due to the microstructure of QAPS is almost similar to Nafion. It represents that the Nafion membrane is compatible with QAPS membrane. If the membranes are not compatible to each other, the performance will be degraded, causing flooding issue, and stability of membrane decrease. To the best of our knowledge, none of the research has discussed the importance of membrane compatibility on cell performance.

- Fabrication and operating conditions of BPMFC

The BPM should be fabricated at the appropriate membrane thickness to decrease its ionic resistance. The suitable membrane thickness can be determined by testing the cell at different thickness. A previous study had determined the influence of AEM thickness on power output, but not for PEM. This is because ORR occurs at the AEM side and it suggested that more attention should be given on AEM, rather than PEM side. However, it is no doubt that PEM also plays an important role in PEMFC because it transports hydrogen ion to the junction layer. Hence, the wrong choice of thickness for PEM will affect the effectiveness of proton transport. Besides that, the operating conditions, such as humidity of  $\text{H}_2$  and  $\text{O}_2$  gases, operating temperature of fuels, air pressure and the stoichiometric flow rate of air should also be controlled and chosen carefully before testing the BPMFC.

### Acknowledgment

The authors are thankful to Universiti Teknologi Malaysia for generous financial sponsorship under Zamalah Scholarship to support one of the authors, i.e. Syarifah Noor Syakiylla Sayed Daud and Ministry of Education for providing fund for this study (Vot 4J207).

### References

- [1] Bhatt S, Gupta B, Sethi V K and Pandey M 2012 Polymer Exchange Membrane ( PEM ) Fuel Cell: A Review *Int. J. Current and Tech.* **2** 219
- [2] Daud W R W, Rosli R E, Majlan E H, Hamid S A A, Mohamed R and Husaini T 2017 PEM Fuel Cell System Control: A Review *Renewable Energy* **113** 620
- [3] Pu H 2014 *Polymer for PEM Fuel Cells*. Hoboken, New Jersey: John Wiley and Sons
- [4] Ahmed N A, Miyatake and Al-Othman A K 2008 Power Fluctuations Suppression of Stand-alone Hybrid Generation Combining Solar Photovoltaic/wind Turbine and Fuel Cell Systems *Energy Convers. Manag.* **49** 2711
- [5] Jacobson M Z 2010 Short-term Effects of Controlling Fossil-fuel Soot, Biofuel Soot and Gases, and Methane on Climate, Arctic Ice, and Air Pollution Health *J. Geophys. Res. Atmos.* **115** 1
- [6] Saadi A, Becherif M, Hissel D and Ramadan H S 2016 Dynamic Modeling and Experimental Analysis of PEMFCs: A Comparative Study *Int. J. Hydrogen Energy* **42** 1
- [7] Tan J, Chao Y J, Van Zee J W, Li X, Wang X and Yang M 2008 Assessment of Mechanical Properties of Fluoroelastomer and EPDM in A Simulated PEM Fuel Cell Environment by Microindentation Test *Mater. Sci. Eng. A* **496** 464
- [8] Nguyen M D T, Dang H S and Kim D 2015 Proton Exchange Membranes Based on Sulfonated Poly(arylene ether ketone) Containing Triazole Group for Enhanced Proton Conductivity *J. Memb. Sci.* **496** 13
- [9] Smitha B, Devi D A and Sridhar S 2008 Proton-conducting Composite Membranes of Chitosan and Sulfonated Polysulfone for Fuel Cell Application *Int. J. Hydrogen Energy* **33** 4138
- [10] Bazylak A 2009 Liquid Water Visualization in PEM Fuel Cells: A Review *International Journal of Hydrogen Energy* **34** 3845
- [11] Alink R and Gerteisen D 2013 Modeling The Liquid Water Transport in The Gas Diffusion Layer for Polymer Electrolyte Membrane Fuel Cells using A Water Path Network *Energies* **6** 4508
- [12] Long R, Chen Q, Zhang L, Ma L, and Quan S 2013 Online Soft Sensor of Humidity in PEM Fuel Cell Based on Dynamic Partial Least Squares *Scientific World Journal* (2013)923901
- [13] Tüber K, Pócza D and Hebling C 2003 Visualization of Water Buildup In the Cathode of A Transparent PEM Fuel Cell *J. Power Sources* **124** 403
- [14] Li H, Tang Y, Wang Z, Shi Z, S. Wu et al 2008 A Review of Water Flooding Issues in The Proton Exchange Membrane Fuel Cell *J. Power Sources* **178** 103
- [15] Ashrafi M and Shams M 2017 The Effects of Flow-field Orientation on Water Management in PEM Fuel Cells with Serpentine Channels *Appl. Energy* **208** 1083
- [16] Park J, Oh H, Lee Y, Min K, Lee E and Jyoung J Y 2016 Effect of The Pore Size Variation in The Substrate of The Gas Diffusion Layer on Water Management and Fuel Cell Performance *Appl. Energy* **171** 200
- [17] Blanco M and Wilkinson D P 2014 Investigation of The Effect of Microporous Layers on Water Management in A Proton Exchange Membrane Fuel Cell using Novel Diagnostic Methods *International Journal of Hydrogen Energy* **39** 16390
- [18] Bacon 2000 Bipolar Membrane Technology And Its Applications *Membr. Technol.* **125** 8
- [19] Tongwen X 2002 Electrodialysis Processes with Bipolar Membranes (EDBM) In Environmental Protection - A review *Resour. Conserv. Recycl.* **37** 1
- [20] Chang Y, Qin Y, Yin Y, Zhang J and Li X 2018 Humidification Strategy for Polymer Electrolyte Membrane Fuel Cells – A Review *Applied Energy* **230** 643

- [21] Ünlü M, Zhou J and Kohl P A 2009 Hybrid Anion and Proton Exchange Membrane Fuel Cells *J. Phys. Chem. C* **113** 11416
- [22] Peng S, Xu X, Lu S, Sui P C, Djilali N and Xiang Y 2015 A Self-humidifying Acidic-alkaline Bipolar Membrane Fuel Cell *J. Power Sources* **299** 273
- [23] Shen W, Prasad A K and Hertz J L 2011 A Non-flooding Hybrid Polymer Electrolyte Fuel Cell *Electrochem. Solid-State Lett.* **14** B121
- [24] Arges C G, Prabhakaran V, Wang L and Ramani V 2014 Bipolar Polymer Electrolyte Interfaces for Hydrogen-oxygen and Direct Borohydride Fuel Cells *Int. J. Hydrogen Energy* **39** 14312
- [25] He W S, Lin G Y and Nguyen T V 2003 Diagnostic Tool to Detect Electrode Flooding in Proton-Exchange-Membrane Fuel Cells *AIChE J* **49** 3221
- [26] Ge S, Yi B, and Ming P 2006 Experimental Determination of Electro-Osmotic Drag Coefficient in Nafion Membrane for Fuel Cells *J. Electrochem. Soc.* **153** A1443
- [27] Gholizadeh M, Ghazikhani M and Khazaei I 2016 Effect of Changing The Water Balance on Electro-Osmotic Flow in An Elliptical Single Proton Exchange Membrane Fuel Cell *Energy Convers. Manag.* **120** 44
- [28] Springer T E, Zawodzinski T A, and Gottesfeld S 1991 Polymer Electrolyte Fuel Cell Model *J. Electrochem. Soc.* **138** 2334
- [29] Peng S, Lu S, Zhang J, Sui P C and Xiang Y 2013 Evaluating The Interfacial Reaction Kinetics of The Bipolar Membrane Interface in The Bipolar Membrane Fuel Cell *Phys. Chem. Chem. Phys.* **15** 11217
- [30] Li Q, Gong J, Peng S, Lu S, Sui P C, Djilali N and Xiang Y 2016 Theoretical Design Strategies of Bipolar Membrane Fuel Cell with Enhanced Self-Humidification Behavior *J. Power Sources* **307** 358
- [31] Awang N, Ismail A F, Jaafar J, Matsuura T, Junoh H, Othman M H D and Rahman M A 2015 Functionalization Of Polymeric Materials as A High Performance Membrane for Direct Methanol Fuel Cell: A Review *Reactive and Functional Polymers* **86** 248
- [32] Othman M H D, Jaafar J, Ismail A F, Matsuura T, Rahman M A, Awang N and Junoh H 2014 Functionalization of Polymeric Materials as A High Performance Membrane for Direct Methanol Fuel Cell: A Review *React. Funct. Polym.* **86** 248
- [33] Ran J, Wu L, He Y, Yang Z, Wang Y et al. 2017 Ion Exchange Membranes :New Developments and Applications *J. Memb. Sci.* **522** 267
- [34] Ge L, Ran J, He Y, Wang Y, Xu T et al. 2016 Ion Exchange Membranes: New Developments and Applications *J. Memb. Sci.* **522** 267
- [35] Charles J, Carraher E 2010 *Introduction to Polymer Chemistry* 2nd ed. Boca Raton, United States of America: Taylor and Francis Group
- [36] Majsztrik P W 2008 Mechanical and Transport Properties of Nafion for PEM Fuel Cells; Temperature and Hydration Effects *Appl. Evol. Comput. Chem.* **141** 235
- [37] Shaari N and Kamarudin S K 2019 Recent Advances in Additive-Enhanced Polymer Electrolyte Membrane Properties in Fuel Cell Applications: An Overview *International Journal of Energy Research* (2019)1
- [38] Choi J S, Sohn J Y and Shin J A 2015 Comparative Study on EB-Radiation Deterioration of Nafion Membrane in Water and Isopropanol Solvents *Energies* **8** 5370
- [39] Choi B, Langlois D A, Mack N, Johnston C M and Kim Y S 2014 The Effect of Cathode Structures on Nafion Membrane Durability *J. Electrochem. Soc.* **161** F1154
- [40] Paddison S and Zawodzinski T A J 1998 Molecular Modeling of The Pendant Chain in Nafion® *Solid State Ionics* **115** 333
- [41] Mauritz K A and Moore R B 2004 State of Understanding of Nafion *Chem. Rev.* **104** 4535
- [42] Barbir F 2015 *Fuel Cell Technology Reaching Towards Commercialization* Springer, New York City: United States
- [43] Liu W, Ruth K and Rusch G Membrane 2001 Durability in PEM Fuel Cells *J. New Mater. Electrochem. Syst.* **4** 227

- [44] Chen T Y and Leddy J 2000 Ion Exchange Capacity of Nafion and Nafion Composites *Langmuir* **16** 2866
- [45] Li H Y and Liu Y L 2014 Nafion-Functionalized Electrospun Poly(Vinylidene Fluoride) (PVDF) Nanofibers for High Performance Proton Exchange Membranes in Fuel Cells *J. Mater. Chem. A* **2** 3783
- [46] Tang H L and Pan 2008 M Synthesis and Characterization of A Self-Assembled Nafion/Silica Nanocomposite Membrane for Polymer Electrolyte Membrane Fuel Cells *J. Phys. Chem. C* **112** 11556
- [47] Liu Y L, Su Y, Chang H, Suryani C M, Wang D M and Lai J Y 2010 Preparation and Applications of Nafion-Functionalized Multiwalled Carbon Nanotubes for Proton Exchange Membrane Fuel Cells *J. Mater. Chem.* **20** 4409
- [48] Damay F and Klein L C 2003 Transport Properties of Nafion<sup>™</sup> Composite Membranes for Proton-Exchange Membranes Fuel Cells *Solid State Ionics* **162** 261
- [49] Yu T L, Lin H L, Shen K S, Huang L N, Chang Y C, Jung G B and Huang J C 2004 Nafion/PTFE Composite Membranes for Fuel Cell Applications *J. Polym. Res.* **11** 217
- [50] Collette F M, Lorentz C, Gebel G and ThomINETTE F 2009 Hygrothermal Aging of Nafion<sup>®</sup> *J. Memb. Sci.* **330** 21
- [51] Iulianelli A and Basile A 2012 Sulfonated PEEK-based Polymers in PEMFC and DMFC Applications: A Review *Int. J. Hydrogen Energy* **37** 15241
- [52] Arges C G, Kulkarni S, Mauritz K A, Patton D, Baranek A, Ramani V, Pan K J, and Jung M S 2010 Quarternary Ammonium and Phosphonium Based Anion Exchange Membranes for Alkaline Fuel Cells *The Electrochemical Socie.* **33** 1903
- [53] Zhu L, Tian D, Shin D, Jia W, Bae C and Lin H 2018 Effects of Tertiary Amines and Quaternary Ammonium Halides in Polysulfone on Membrane Gas Separation Properties *J. Polym. Sci. Part B Polym. Phys.* **56** 1239
- [54] Roddecha S, Dong Z, Wu Y and Anthamatten M 2012 Mechanical Properties and Ionic Conductivity of Electrospun Quaternary Ammonium Ionomers *J. Memb. Sci.* **389** 478
- [55] Abuin G C, Nonjola P, Franceschini E A, Izraelevitch F H, Mathe M K and Corti H R 2010 Characterization of An Anionic-Exchange Membranes for Direct Methanol Alkaline Fuel Cells *Int. J. Hydrogen Energy* **35** 5849
- [56] Tang H, Li D, Li N, Zhang Z and Zhang Z 2018 Anion Conductive Poly(2,6-Dimethyl Phenylene Oxide)s with Clicked Bulky Quaternary Phosphonium Groups *J. Memb. Sci.* **558** 9
- [57] Yan X, Gu S, He G, Wu X, Zheng W and Ruan X 2014 Quaternary Phosphonium-Functionalized Poly(Ether Ether Ketone) as Highly Conductive and Alkali-Stable Hydroxide Exchange Membrane for Fuel Cells *J. Memb. Sci.* **466** 220
- [58] Jiang L, Lin X, Ran J, Li C, Wu L and Xu T 2012 Synthesis and Properties of Quaternary Phosphonium-Based Anion Exchange Membrane for Fuel Cells *Chinese J. Chem.* **30** 2241
- [59] Xu T, Ran J, Li C, Jiang L, Lin X and Wu 2012 Synthesis and Properties of Quaternary Phosphonium-based Anion Exchange Membrane for Fuel Cells *Chinese J. Chem.* **30** 2241
- [60] Sun Z, Pan J, Guo J and Yan J 2018 The Alkaline Stability of Anion Exchange Membrane for Fuel Cell Applications: The Effects of Alkaline Media *Adv. Sci.* **5** 1
- [61] Hossain M A, Jang H, Lim Y, Lee S, Joo H, Hong T, Tan F and Kim W G 2014 Anion Conductive Imidazolium-based Parmax Alkaline Membrane for Fuel Cell Applications *IREC 2014 - 5th International Renewable Energy Congress 25-27 March, Hammamet, Tunisia* 1
- [62] Lin B, Qiao G, Chu F, Wang J, Feng T, Yuan N, Zhang S, Zhang X and Ding J 2017 Preparation and Characterization of Imidazolium-Based Membranes for Anion Exchange Membrane Fuel Cell Applications *Int. J. Hydrogen Energy* **42** 6988
- [63] Li W, Fang J, Lv M, Chen C, Chi X, Yang Y and Zhang Y 2011 Novel Anion Exchange Membranes Based on Polymerizable Imidazolium Salt for Alkaline Fuel Cell Applications *J. Mater. Chem.* **21** 11340
- [64] Lu W, Shao Z G, Zhang G, Zhao Y, Li J and Yi B 2013 Preparation and Characterization of

- Imidazolium-Functionalized Poly (Ether Sulfone) as Anion Exchange Membrane and Ionomer for Fuel Cell Application *Int. J. Hydrogen Energy* **38** 9285
- [65] Song Y, Liu C, Zhao J and Luo J 2016 Imidazolium-functionalized Anion Exchange Polymer Containing Fluorine Group for Fuel Cell Application *International Journal of Hydrogen Energy* **41** 10446
- [66] Yan X, Gao L, Zheng W, Ruan X, Zhang C, Wu X and He G 2016 Long-spacer-chain Imidazolium Functionalized Poly(Ether Ether Ketone) as Hydroxide Exchange Membrane for Fuel Cell *Int. J. Hydrogen Energy* **41** 14982
- [67] Jang H, Hossain M A, Sutradhar S C, Ahmed F, Choi K, Ryu T, Kim K and Kim W 2017 Anion Conductive Tetra-sulfonium Hydroxides Poly(fluorenylene ether sulfone) Membrane for Fuel Cell Application *Int. J. Hydrogen Energy* **42** 12759
- [68] Hossain M A, Jang H, Sutradhar S C, Ha J, Yoo J, Lee C, Lee S and Kim W 2016 Novel Hydroxide Conducting Sulfonium-based Anion Exchange Membrane for Alkaline Fuel Cell Applications *International Journal of Hydrogen Energy* **41** 10458
- [69] Sutradhar S C, Yoo J, Lee S, Kim W, Hossain M A, Ha J, Jang H and Lee C 2016 Novel Hydroxide Conducting Sulfonium-Based Anion Exchange Membrane for Alkaline Fuel Cell Applications *Int. J. Hydrogen Energy* **41** 10458
- [70] Lin X, Wu L, Liu Y, Ong A L, Poynton S D, Varcoe J R and Xu T 2012 Alkali Resistant and Conductive Guanidinium-based Anion-Exchange Membranes for Alkaline Polymer Electrolyte Fuel Cells *J. Power Sources* **217** 373
- [71] Jasti A, Prakash S and Shahi V K 2013 Stable and Hydroxide Ion Conductive Membranes for Fuel Cell Applications: Chloromethylation and Amination of Poly(Ether Ether Ketone) *J. Memb. Sci.* **428** 470
- [72] Merle G, Wessling M and Nijmeijer 2011 Anion Exchange Membranes for Alkaline Fuel Cells: A Review *Journal of Membrane Science* **377** 1
- [73] Couture G, Alaaeddine A, Boschet F and Ameduri B 2011 Polymeric Materials as Anion-Exchange Membranes for Alkaline Fuel Cells *Prog. Polym. Sci.* **36** 1521
- [74] McClure J, Grew K and Chu D 2015 Experimental Development of Alkaline and Acid-Alkaline Bipolar Membrane Electrolytes *Electrochem. Soc.* **69** 35
- [75] Ünlü M, Zhou J and Kohl P A 2010 Self Humidifying Hybrid Anion-cation Membrane Fuel Celloperated under Dry Conditions *Fuel Cells* **10** 54
- [76] Arges C G, Wang L, Parrondo J and Ramani V 2013 Best Practices for Investigating Anion Exchange Membrane Suitability for Alkaline Electrochemical Devices: Case Study Using Quaternary Ammonium Poly(2,6-dimethyl 1,4-phenylene)oxide Anion Exchange Membranes *J. Electrochem. Soc.* **160** F1258
- [77] Tongwen X and Weihua Y 2001 Fundamental Studies of A New Series Of Anion Exchange Membranes: Membrane Preparation and Characterization *J. Memb. Sci.* **190** 159